Disease-Aware Chest X-Ray Style GAN Image Generation and CatBoost Gradient Boosted Trees

Andi Besse Firdausiah Mansur
Faculty of Computing and Information Technology in Rabigh, Jeddah, Saudi Arabia

***Abstract*—Artificial Intelligence has significantly advanced and is proficient in image classification. Even though the COVID-19 pandemic has ended, the virus is now considered to have entered an endemic phase. Historically, COVID-19 detection has predominantly depended on a single technology known as the polymerase chain reaction (PCR). The academic community is keen radiograph data to forecast COVID-19 because of its prospective advantages. The proposed methodology aims to improve dataset quality by utilizing artificially generated images produced by StyleGAN. The ratio of 59:41 was used to combine the synthetic datasets with the real ones. The combination of the StyleGAN framework, the VGG19, and CatBoost Gradient Boosted Trees is to improve prediction accuracy. Accurate and precise measurements significantly impact the evaluation of a model's performance. The assessment resulted in 98.67% accurate and 97.21% precise. In the future, we may enhance the diversity and quality of the collection by integrating other datasets from different sources with the Chest X-ray dataset.**

Keywords*—*Artificial intelligence; StyleGAN; chest X-ray prediction; COVID19; CatBoost gradient boosted trees

I. Introduction

COVID-19, a respiratory infection commonly known as the coronavirus, has significantly affected a large portion of the global population. The latest statistics show that there have been over 243 million global infections to date. Saudi Arabia has reported over 801,000 cases of COVID-19 with a mortality rate of about 1.15%, resulting in 9,223 deaths [1,2]. Despite widespread vaccination, health precautions must still be adhered to as directed by health authorities. COVID-19 presents several symptoms including high fever, vomiting, and diarrhea. X-ray images can provide a comprehensive diagnosis to observe viruses' effects on toward human. Analyzing COVID-19 through visual inspection of X-ray pictures has open great chance to utilize artificial intelligence to thoroughly study infection areas and maybe forecast future spread. Convolutional neural networks (CNNs) are recognized as an effective method for detecting and identifying medical pictures [3,4].

Because of the nature of the requirements for autonomous disease diagnoses and faster processing with large output, the research on image analysis for chest X-rays continues to be fascinating.

In previous research, the analysis of the chest X-ray data was carried out utilizing a variety of deep learning techniques and different classifiers. Our approach, on the other hand, is distinct because we utilized the StyleGAN framework in order to enhance the quality and variety of the dataset.

These are the key components that were found in the research result, and they can be described as the primary results of this study:

1) Data augmentation was used to enhance the quality of the dataset by using various image preprocessing techniques, such as rotation, scaling, and flipping. The styleGAN framework was then used to build the dataset with the variety model, enhancing both the amount and diversity of the chest X-ray image dataset. The usage of computing resources is a limitation of styleGAN. This is due to the fact that larger images demand high-end GPU computation. Because of this, it is necessary to reduce the size of the photos at various points during the tuning process.

2) The handling of StyleGAN picture data was accomplished with the help of a VGG19 model, which resulted in higher accuracy rates than those achieved by earlier studies. Better feature mapping can be achieved by the application of the CatBoost Gradient Boosted Trees approach.

Following is the structure of the remaining parts of this paper: Section II offers a comprehensive summary of the works that are linked to this topic. Section III provides an illustration of the methodology that is utilized in the proposed model. In Section IV, the experimental performance results together with the descriptions of the dataset are offered. A concise analysis of the proposed research is presented in Section V of the document. Within Section VI, the conclusion and recommendations for the future are presented.

II. Related Works

The GAN framework for image recognition has been used widely for medical image processing approaches. The previous research proposed system that based on Generative adversial network to produce fake image classification using Forward and Backward GAN [5]. GAN also showed its effectiveness in detecting anomalies in retinal images to compare healthy and unhealthy ones. Therefore, the lack of a dataset has driven researchers to do more exploration on the dataset. Therefore, such a Generative Adversarial Network (GAN) technique is needed to overcome the dataset's limitation [6-8]. In recent research in the Journal of Radiology, X-ray chest imagery is superior to outclassed lab testing such as PCR or rapid tests. Consequently, many researchers resolved that chest radiography detection should be used as the primary screening method for COVID-19 infection detection. Radiography images combined with AI [5, 9]. It can do massive detection and ease the work of doctors and nurses so they can use energy to treat positive patients. Computers have a significant role in diagnosing diseases. However, it can be used for measuring the chronicness and complications of the patients [7].

The model was utilized to conduct an analysis of confirmed instances of COVID-19 that occurred in acute care settings in India [10]. Through the utilization of chest X-ray images and the application of metaheuristic algorithms, K. Shankar and his colleagues developed a fusion model for the diagnosis of COVID-19 [11]. Curating a medical picture collection is a costly and laborious task that involves the collaboration of radiologists and researchers. CNNs excel at these tasks because of their extensive parameters and meticulous fine-tuning methodology. Despite having limited datasets, it is capable of performing the most effective detection and recognition process [12-14].

Utilizing this method, it allows for the incorporation of a modified dataset into the training process. Through the course of the epidemic, it has become increasingly popular to employ artificial intelligence (AI) that is equipped with deep learning capabilities in order to analyze chest X-ray pictures. The objective of this project is to develop a research technique that will enable anomalies to be identified in their radiograph pictures. Artificial intelligence was utilized by another researcher in order to identify COVID-19 through the use of coughy sounds. In order to identify and diagnose respiratory illnesses, the researchers concentrated their efforts on analyzing cough sounds coming from a variety of sources. By utilizing a support vector machine (SVM) classifier in conjunction with linear regression techniques, this was successfully accomplished. For the purpose of analyzing cough patterns and determining the severity of respiratory problems in patients, artificial neural networks (ANNs) and the random forest (RF) classifier are utilized. It is possible to identify respiratory issues such as asthma and cough by employing Wigner distribution methods in an atmosphere that is free from sounds [15-19].

In order to train on specific datasets, they made use of transfer learning models that involved two steps [20]. During the first stage of their project, they utilized a deep residual network that had been pre-trained on a big dataset pertaining to pneumonia. COVID-19 was successfully detected in X-ray images of healthy individuals as well as individuals who were sick with pneumonia. Past studies have employed several methods for data augmentation, including picture alteration, color adjustment, distortion, and enhancement [21]. An individual infected with COVID-19 may exhibit several symptoms, including fever and a cough like those of influenza. Severe cases can result in organ failure, respiratory distress, and mortality [22, 23].

Due to the rapid increase in COVID-19 cases, numerous countries are experiencing significant challenges with their healthcare systems, with many on the brink of collapse due to insufficient capacity to accommodate a high volume of patients simultaneously [24, 25]. In the past PCR is highly used as core of COVID 19 detection and even used as standard for travel requirements [26, 27]. This is sometimes referred to as a swab test. Collecting nasal or throat fluid may yield results within a few hours or days. Additionally, another method involves acquiring X-ray radiography images of the patient's chest [34].

III. Material and Method

This section will focus on delivering the core idea of dataset generation using style GAN and CATBoost Gradient algorithm for Generating Chest X-ray Image.

A. Chest X-Ray Dataset

Research in the field of academia has traditionally concentrated on binary classification of binary images. The Paul Cohen dataset, which has a number of different resolutions, was used to collect data from a range of sources, including healthy persons as well as patients who were diagnosed with pneumonia (see Fig. 1) [28].

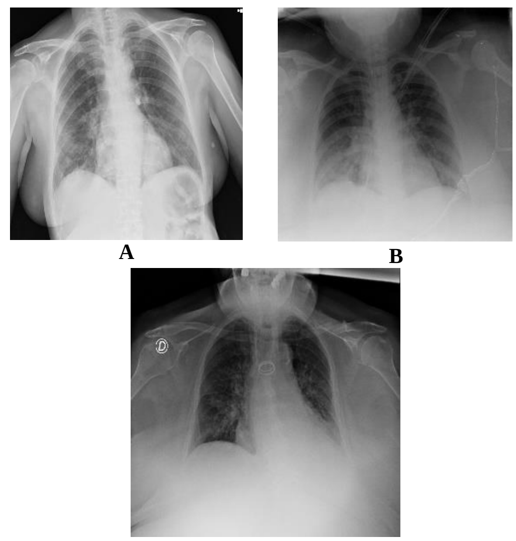

Fig. 1. Chest X-Ray dataset:A: Normal, B: Pneumonia, C:COVID-19.

B. Style GAN Image Generator

Style GAN generator modify the input layer with learning constant. The generator incorporates the input latent code into an intermediate latent space, significantly influencing how the network represents the factors of variation. The latent space input should adhere to the probability density of the training data, resulting in inevitable entanglement to some extent [29]. A non-linear mapping network, denoted as $f : Z \rightarrow W$, initially generates $w \in W$ from a latent code z in the input latent space, first transform the input into an intermediate latent space W, which subsequently regulates the generator using adaptive instance normalization (AdaIN) at every convolution layer. Gaussian noise is incorporated following each convolution, prior to assessing the nonlinearity. The detail diagram is shown in Fig. 2.

"A" represents a trained affine transformation, whereas "B" implements trained per-channel scaling factors on the noise input. Network f comprises eight layers, while network g comprises 18 layers. The AdaIN process is defined in Eq. (1).

$$AdaIN(x_i, y) = y_{s,i} \frac{x_i - \mu(x_i)}{\sigma(x_i)} + y_{b,i} \tag{1}$$

Each feature map x_i is individually normalized, then adjusted and offset using the matching scalar components from style y. The dimensionality of y is equal to two times the number of feature mappings on that layer.

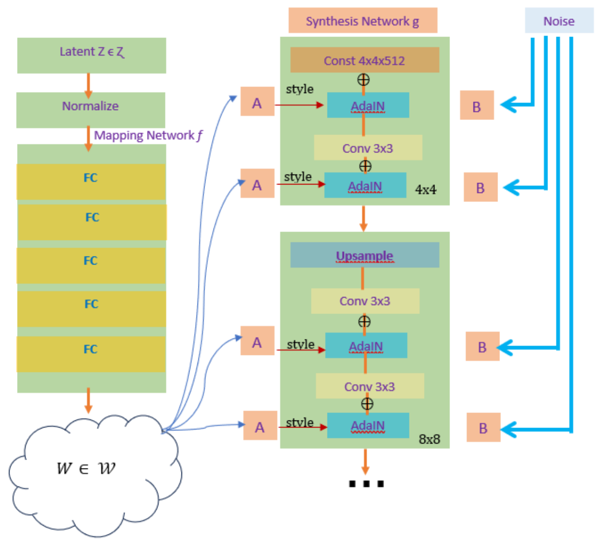

Fig. 2. Re-illustration of styleGAN architecture from Karras, T. et al [29].

C. CatBoost Gradient Boosted Trees

In supervised machine learning, we start with a set of input values [7] and their corresponding expected output values $y_i, i \in \{1 \dots n\}$, where i ranges from 1 to n. Gradient boosting incrementally builds a series of functions F^0, F^1, ..., F^t, ..., F^m, based on a loss function $\mathcal{L}(y_i, F^t)$. We want to highlight that $\mathcal{L}$ contains two input values: the *i*th expected output value y_i and the *t*th function F^t estimates y_i.

Once function F^t is established, we can enhance our predictions of y_i by determining another function $F^{t+1} = F^t + h^{t+1}(x)$ that minimizes the expected value of the loss function, as depicted in Eq. 2 [30].

$$h^{t+1} = \underset{h \in H}{argmin} \mathbb{E}\mathcal{L}(y, F^t) \tag{2}$$

H represents the set of candidate Decision Trees being assessed to select one for inclusion in the ensemble. Moreover, based on the definition of F^{t+1}, we may express the expected value of the loss function $\mathcal{L}$ using F^t and h^{t+1}, as depicted in Eq. 3.

$$\mathbb{E}\mathcal{L}(y, F^{t+1}) = \mathbb{E}\mathcal{L}(y, F^t + h^{t+1}) \tag{3}$$

The right-hand side of Eq. (3) suggests a desire to reduce the loss function's value on y and F^t, along with an additional component. If we assume that $\mathcal{L}$ is continuous and differentiable, we can incorporate information about the rate of change of $\mathcal{L}$ into F^t to adjust its value in the direction of $\mathcal{L}$'s decrease. Thus, by setting h^{t+1} to values that align with the steepest decrease in the gradient of $\mathcal{L}$ with respect to F^t, we can obtain h^{t+1} that minimizes $\mathbb{E}\mathcal{L}(y, F^t + h^{t+1})$. Given these conditions, we may get a practical estimate for h^{t+1}, as given by Eq. 4.

$$h^{t+1} \approx \underset{h \in H}{argmin} \mathbb{E}\left(\frac{\partial \mathcal{L}_y}{\partial F^t} - h\right)^2 \tag{4}$$

This technique is called Gradient Boosting because it involves utilizing the partial derivatives (gradients) of the loss function $\mathcal{L}$ in relation to the function F^t to determine h^{t+1}. Prokhorenkova et al. [31] highlight the challenge of computing $\underset{h \in H}{argmin} \mathbb{E}\left(\frac{\partial \mathcal{L}_y}{\partial F^t} - h\right)^2$. It may be challenging to determine the likelihood of specific values of $\underset{h \in H}{argmin} \mathbb{E}\left(\frac{\partial \mathcal{L}_y}{\partial F^t} - h\right)^2$ due to the usage of stochastic techniques such algorithms for constructing Decision Trees to define F^t. Therefore the equation might be modified as depicted in Eq. (5) [30].

$$\underset{h \in H}{argmin} \mathbb{E}\left(\frac{\partial \mathcal{L}_y}{\partial F^t} - h\right)^2 \approx \underset{h \in H}{argmin} \frac{1}{n}\left(\frac{\partial \mathcal{L}_y}{\partial F^t} - h\right)^2 \tag{5}$$

We are discussing Friedman's Gradient Boosting Decision Trees technique in this section, however we refer to [31] in our explanation to ensure the reader gains a good understanding of CatBoost. To calculate an accurate estimate for h^{t+1}, we can use approximations Eq. (4) and Eq. (5), so the equation can be finalized as Eq. (6).

$$h^{t+1} \approx \underset{h \in H}{argmin} \frac{1}{n}\left(\frac{\partial \mathcal{L}_y}{\partial F^t} - h\right)^2 \tag{6}$$

CatBoost employs a more efficient approach that minimizes overfitting and enables the utilization of the entire dataset for training [32]. A randomly shuffle the dataset and calculate the average label value for each example based on the examples with the same category value that come before it in the shuffled order. If $\sigma = (\sigma_1, \dots, \sigma_n)$ be the permutation, then $x_{\sigma_p,k}$ is replaced by Eq. (7).

$$\frac{\sum_{j=1}^{p-1}\left[x_{\sigma_j,k} = x_{\sigma_p,k}\right] Y_{\sigma_p} + a \cdot P}{\sum_{j=1}^{p-1}\left[x_{\sigma_j,k} = x_{\sigma_p,k}\right] Y_{\sigma_p} + a \cdot} \tag{7}$$

We include a previous value P and a parameter a > 0, which represents the weight of the prior. Utilizing a prior is a popular method that aids in diminishing the noise derived from low-frequency categories. The conventional method for determining the prior in regression problems is to get the average label value in the dataset.

CatBoost can create s random permutations of our training dataset. To improve the algorithm's resilience, we utilize many permutations by randomly sampling one and calculating gradients based on it. These permutations are identical to the ones employed in statistical analysis of categorical characteristics. Utilizing several permutations for training different models prevents overfitting. We train n distinct models for every permutation σ, as demonstrated below. The model includes a distinct model called M_k, which remains static and is not updated using a gradient estimate for this particular example.

The estimation of gradient on X_k using M_k and utilize this estimate to evaluate the resulting tree. Here is the pseudo-code that illustrates how to do this trick. The optimal loss function is denoted as Loss(y, α), where y represents the label value and

α represents the formula value, as explained in Algorithm 1 [32].

Algorithm 1: Gradient estimation Calculation

Input: $\left\{(X_k,(Y_k))_{k=1}^{n}\right.$ sorted by σ, the quantity of trees I; $\left.\right\}$
$M_i \leftarrow 0$ *for* $i = 1 \dots n$;
for iter ← 1 to I **do**
  for i ← 1 to n **do**
    for j ← 1 to i-1 **do**
      $g_j \leftarrow \frac{d}{d\alpha} Loss(y_j, \alpha)| \ \alpha = M_i(X_j)$;
    M ←LearnOneThree$((x_j, g_j)$ *for* $j = 1 \dots i-1)$;
    $M_i \leftarrow M_i + M$;
return $M_1 \dots M_n$; $M_1(\boldsymbol{X}_1), M_2(\boldsymbol{X}_2), M_n(\boldsymbol{X}_n)$

CatBoost generates random permutations for our training dataset. We utilize several permutations to strengthen the algorithm's robustness. It will then utilize a random permutation sample to obtain gradients based on it. These permutations are identical to those utilized in statistical calculations for categorical attributes. Training unique models with various permutations does not result in overfitting. The training of n distinct models Mi for each permutation σ. For constructing a single tree, O(n^2) approximations need to be stored and recalculated for each permutation σ. This involves updating Mi(X1), ., Mi(Xi) for each model Mi.

IV. Result

This section details the implementation and outcomes of creating Chest X-ray pictures using the StyleGAN technique, VGG19, and CatBoost Gradient Boosted Tree.

A. StyleGAN Chest X-Ray Image Reconstruction

The StyleGAN technique is employed to create a new dataset by including elements from the original data. Two training components are utilized here:

1) Step 1: Convert the input into an intermediate latent space W, then control the generator by applying adaptive instance normalization (AdaIN) at each convolution layer.

2) Step 2: Gaussian noise is added after each convolution, before analyzing the nonlinearity to create the image.

The technique commences by creating counterfeit images using the StyleGAN methodology. At first glance, the painting appears to be a black canvas. After numerous iterations, the shadow gradually became visible on the chest X-ray scans. After thousands of iterations, the resulting image displayed a recognized chest X-ray image. After more than 5000 repetitions, the created image displayed a visually pleasing outcome, as depicted in Fig. 3.

B. VGG19 Image Classification Results

We utilized single main dataset from Cohen, J.P. [28], together with a dataset created by the StylegGAN technique, as described in the preceding section. When creating an image dataset with DCGAN, the GPU's constraints limit the output to just 100 chest X-ray images in one batch. Analysis of generated images shows that around 59% of the overall dataset is represented by a subset of the StyleGAN data. The collection consists approximately 1500 artificially produced images, covering normal lung states, pneumonia, and COVID-19 instances.

The model has been trained with 5000 datasets consisting of three distinct classes: normal, pneumonia, and COVID-19. We conducted a test on 150 normal patients, 47 pneumonia cases, and 88 COVID-19 cases. We trained our model using VGG19 for 100 epochs with a batch size of 128. The proposed model achieved a training accuracy of 98.89% and a validation accuracy of the same percentage. The validation loss is 0.015. Refer to Fig. 4 for the graph. The graph shows variations during the early phases of training, which are caused by the minimal data available. To resolve this problem and guarantee consistency in the training process, extra data was later included. This instability is common in most TensorFlow training methods.

The classification result is impressive as it accurately categorizes the tested image in comparison to the original dataset. Fig. 5 illustrates the effect of the forecast made by our proposed system. Fig. 5(A) and 5(B) depict the accurate prediction of pneumonia in the original image. Fig. 5(C) was initially normal and is labeled as a normal case, then Fig. 5(D) also describes the correct prediction for COVID 19.

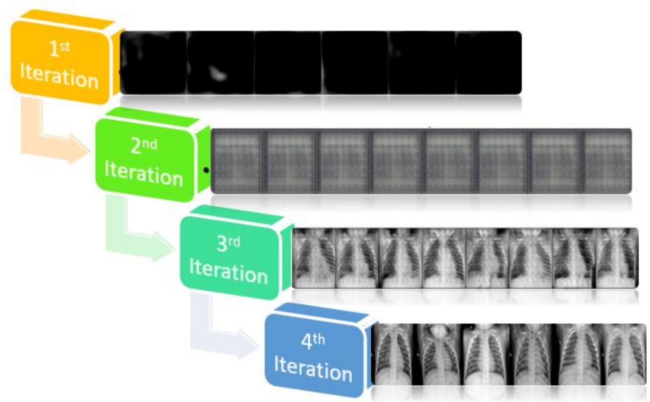

Fig. 3. StyleGAN chest X-ray image reconstruction.

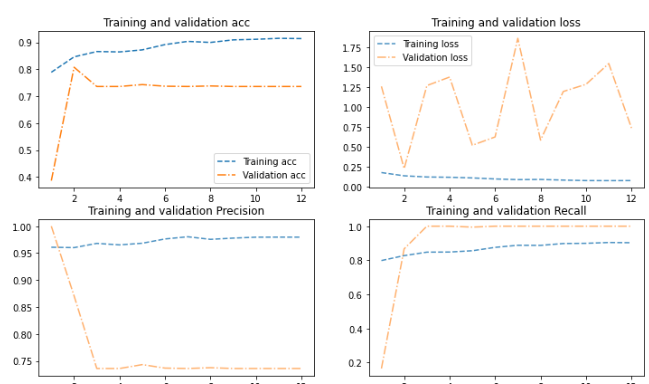

Fig. 4. Training and validation accuracy.

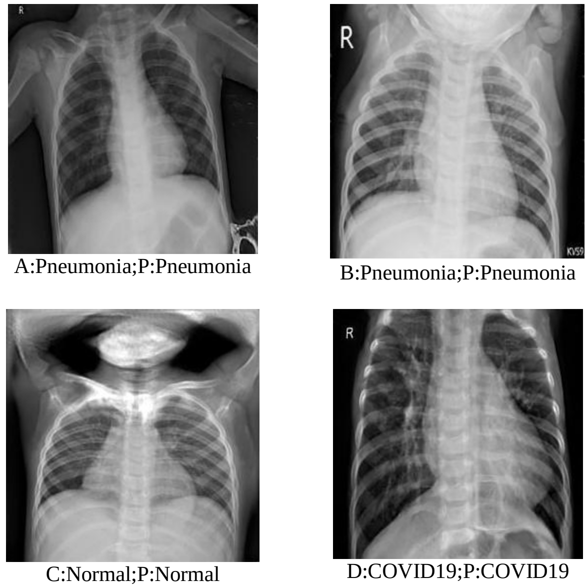

Fig. 5. Classification result.

C. Performance Measurement

Precision, recall, and F1 score are some of the measures that are utilized in the performance evaluation of the individual. These metrics have been defined and are frequently used. The Eq. (8) and (9) include the definitions that are considered to be standard.

$$Precision = \frac{TP}{TP+FP'} \tag{8}$$

$$Recall\ or\ True\ Positive\ Rate = \frac{TP}{TP+FN'} \tag{9}$$

where, FP, FN, TP, and TN are values that correspond to false-positive, false-negative, true-positive, and true-negative, respectively. The F1 score is a metric that is utilized to evaluate the correctness of the model, and it can be calculated by this Eq. (10):

$$F1 = \frac{2 \times precision \times recall}{precision+recall} = \frac{2TP}{2TP+FP+FN'} \tag{10}$$

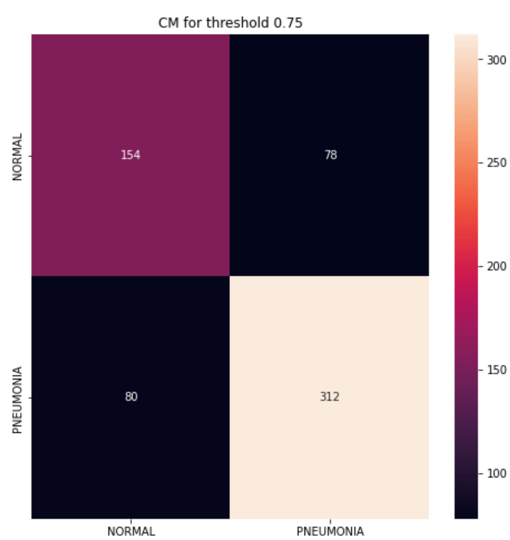

Fig. 6. Confusion matrix of the classification process.

There were approximately 312 cases of pneumonia and 154 cases that were observed to be normal using the confusion matrix, which also revealed good results (see Fig. 6). In addition, the ROC graph demonstrates a positive outcome, as demonstrated by the score of 98.67%, as shown in Fig. 7.

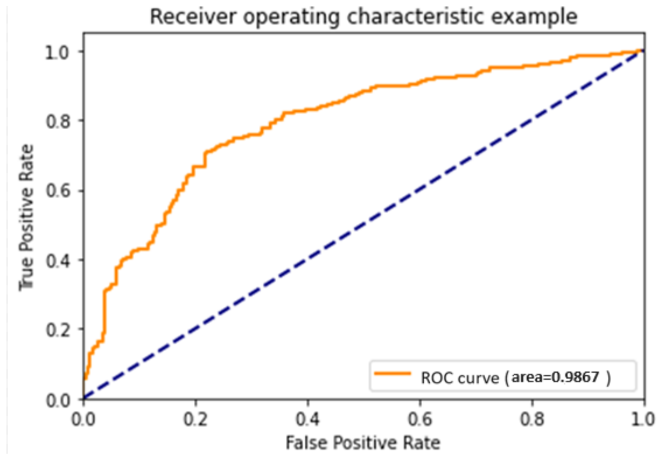

Fig. 7. ROC graph of the classification.

V. Discussion

Within this section, the benchmarking study is presented in comparison to the preceding work. The primary focus of this part is placed on the presentation of comparisons with three previous studies that presented training using a variety of approaches.

Fig. 8 presents a comparison of the performances of the proposed model and its counterparts. It is abundantly clear that the StyleGAN method, when combined with the VGG19 and CatBoost Gradient Boosted Trees model, generates superior augmented images in comparison to the many other methods. The findings are also included in Table I, which compares them to the most recent research.

TABLE I. Classification Benchmarking with Previous Research

Author	Dataset	Method	Accuracy	Precision
Hussain, B.Z., et al [33]	Chest X-ray + Wasserstein GAN	Wasserstein GAN	95.34	99.1
Ciano, G., et al [34]	Chest X-ray + PGGAN	PGGAN + SMANet	96.28	-
Sundaram, S. and N. Hulkund [17]	Chest X-ray + GAN	DenseNet121 + GAN	80.1	72.7
[35]	Chest X-ray + IAGAN	Inception + IAGAN	82	84
Suggested Methodology	Augmented Chest X-Ray with StyleGAN	VGG19 + CatBoost Gradient Boosted Trees	98.67	97.21

According to the data presented in Table I and Fig. 8, the Inception + IAGAN has achieved an accuracy rate of 82% and a precision rate of about 84%. These figures are presented in the format of statistics. When compared to other methods, the PGGAN + SMANet algorithm obtains the best level of accuracy (96.28%), with the Wasserstein GAN algorithm coming in second with a score of 95.34%. This becomes abundantly obvious when the strategy that has been given is contrasted with other methods that are comparable. A precision score of 98.67% and an accuracy rate of 97.21% have been reached by the method that we have presented, which demonstrates that it has generated outstanding results.

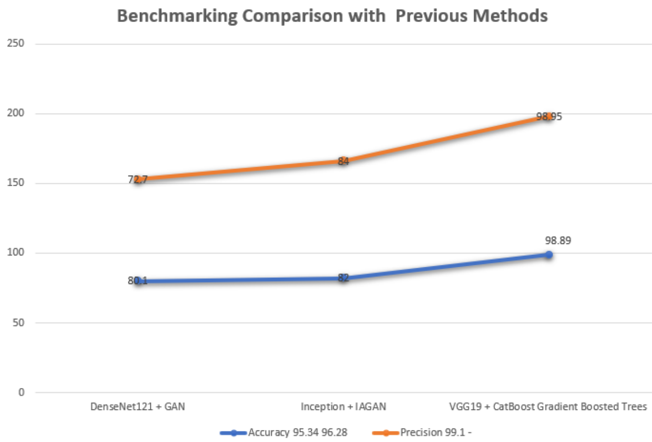

Fig. 8. Benchmarking graph.

VI. Conclusion

Since the COVID-19 pandemic has been brought to an end, it is currently accepted that the virus has transitioned into an endemic phase. This is the case because the pandemic has been concluded. These illnesses have become more widespread to the point where they are a significant source of distress for people of all different demographic groups. This is because the prevalence of these illnesses has increased. Because of the potential that it possesses, the academic community has demonstrated a significant level of interest in the application of radiograph image data in the process of forecasting COVID-19. The methodology that has been provided focuses an emphasis on the employment of images that have been artificially generated by the application of the StyleGAN.

This is done with the intention of improving the overall quality of the datasets. For the purpose of integrating the synthetic datasets with the actual ones, the ratio that was utilized was 59:41. As a consequence of this, a hybrid method was implemented, which included the incorporation of the StyleGAN framework, the VGG19 model, and CatBoost Gradient Boosted Trees. The purpose of this strategy was to enhance the accuracy of the prediction. The evaluation of a model's performance is significantly influenced by the measurements of accuracy and precision that are taken into account on the model. Following are the outcomes of the evaluation, which produced the following results: an accuracy rate of 98.67% and a precision score of 97.21% were the outcomes which were generated. It is possible that the work that will be done in the future will take into consideration the possibility of mixing multiple datasets that have been generated from other sources with the Chest X-ray dataset that has been generated. This will be done with the intention of improving the diversity and quality of the dataset.

Acknowledgment

This work was supported by the Deanship of Scientific Research (DSR), King Abdulaziz University, Jeddah Saudi Arabia. The authors, therefore, gratefully acknowledge the DSR technical and financial support.

References

[1] Health, M.o. Covid19 Command and Control Center CCC, The National Health Emergency Operation Center NHEOC. (2021),https://covid19.moh.gov.sa. 2021 [cited 2021 23 October 2021].

[2] Worldmeter. https://www.worldometers.info/coronavirus. 2021 [cited 2021 23 October].

[3] Wang, S., et al., Cerebral micro‐bleeding identification based on a nine‐layer convolutional neural network with stochastic pooling. Concurrency and Computation: Practice and Experience, 2019. 32.

[4] Wang, S., et al., Cerebral Micro-Bleeding Detection Based on Densely Connected Neural Network. 2019. 13(422).

[5] Zhao, D., et al., Synthetic Medical Images Using F&BGAN for Improved Lung Nodules Classification by Multi-Scale VGG16. Symmetry, 2018. 10(10).

[6] Ahmadinejad, M., et al., Using new technicque in sigmoid volvulus surgery in patients affected by COVID19. Annals of Medicine and Surgery, 2021. 70: p. 102789.

[7] Basha, S.H., et al., Hybrid intelligent model for classifying chest X-ray images of COVID-19 patients using genetic algorithm and neutrosophic logic. Soft Computing, 2021.

[8] Castiglioni, I., et al., Machine learning applied on chest x-ray can aid in the diagnosis of COVID-19: a first experience from Lombardy, Italy. Eur Radiol Exp, 2021. 5(1): p. 7.

[9] Venu, S.K., Evaluation of Deep Convolutional Generative Adversarial Networks for data augmentation of chest X-ray images. A Preprint, Department of Analytics and Data ScienceHarrisburg University of Science and TechnologyHarrisburg, PA 17101,https://arxiv.org/pdf/2009.01181v1.pdf, 2020.

[10] Shastri, S., et al., Deep-LSTM ensemble framework to forecast Covid-19: an insight to the global pandemic. Int J Inf Technol, 2021: p. 1-11.

[11] Shankar, K., et al., Deep learning and evolutionary intelligence with fusion-based feature extraction for detection of COVID-19 from chest X-ray images. Multimed Syst, 2021: p. 1-13.

[12] Greenspan, H., B.v. Ginneken, and R.M. Summers, Guest Editorial Deep Learning in Medical Imaging: Overview and Future Promise of an Exciting New Technique. IEEE Transactions on Medical Imaging, 2016. 35(5): p. 1153-1159.

[13] Roth, H.R., et al., Improving Computer-Aided Detection Using Convolutional Neural Networks and Random View Aggregation. IEEE Transactions on Medical Imaging, 2016. 35(5): p. 1170-1181.

[14] Tajbakhsh, N., et al., Convolutional Neural Networks for Medical Image Analysis: Full Training or Fine Tuning? IEEE transactions on medical imaging, 2016. 35(5): p. 1299-1312.

[15] Singh, M., et al., Transfer learning–based ensemble support vector machine model for automated COVID-19 detection using lung computerized tomography scan data. Medical & Biological Engineering & Computing, 2021. 59(4): p. 825-839.

[16] Soomro, T., et al., Artificial intelligence (AI) for medical imaging to combat coronavirus disease (COVID-19): a detailed review with direction for future research. 2021: p. 1 - 31.

[17] Sundaram, S. and N. Hulkund. GAN-based Data Augmentation for Chest X-ray Classification. in Proceedings of KDD DSHealth, August 14-18, 2021. 2021.

[18] Szegedy, C., et al., Rethinking the Inception Architecture for Computer Vision. Computer Vision and Pattern Recognition, https://arxiv.org/abs/1512.00567v3, 2015.

[19] Tabaa, M., et al., Covid-19's Rapid diagnosis Open platform based on X-Ray Imaging and Deep Learning. Procedia Computer Science, 2020. 177: p. 618-623.

[20] Zhang, R., et al., COVID19XrayNet: A Two-Step Transfer Learning Model for the COVID-19 Detecting Problem Based on a Limited Number of Chest X-Ray Images. Interdisciplinary sciences, computational life sciences, 2020. 12(4): p. 555-565.

[21] Mikołajczyk, A. and M. Grochowski. Data augmentation for improving deep learning in image classification problem. in 2018 International Interdisciplinary PhD Workshop (IIPhDW). 2018.

[22] Mahase, E., Coronavirus covid-19 has killed more people than SARS and MERS combined, despite lower case fatality rate. Bmj, 2020. 368: p. m641.

[23] Wang, W., et al., Detection of SARS-CoV-2 in Different Types of Clinical Specimens. Jama, 2020. 323(18): p. 1843-1844.

[24] Deb, S.D., et al., A multi model ensemble based deep convolution neural network structure for detection of COVID19. Biomedical Signal Processing and Control, 2022. 71: p. 103126.

[25] Degerli, A., et al., COVID-19 infection map generation and detection from chest X-ray images. Health Information Science and Systems, 2021. 9(1): p. 15.

[26] Corman, V.M., et al., Detection of 2019 novel coronavirus (2019-nCoV) by real-time RT-PCR. Euro surveillance: bulletin Europeen sur les maladies transmissibles = European communicable disease bulletin, 2020. 25(3): p. 2000045.

[27] Lal, A., A.K. Mishra, and K.K. Sahu, CT chest findings in coronavirus disease-19 (COVID-19). Journal of the Formosan Medical Association = Taiwan yi zhi, 2020. 119(5): p. 1000-1001.

[28] Cohen, J.P., P. Morrison, and L. Dao, COVID-19 image data collection. arXiv 2003.11597, https://github.com/ieee8023/covid-chestxray-dataset, 2020.

[29] Karras, T., S. Laine, and T. Aila. A Style-Based Generator Architecture for Generative Adversarial Networks. in The Conference on Computer Vision and Pattern Recognition (CVPR). 2019. IEEE.

[30] Hancock, J.T. and T.M. Khoshgoftaar, CatBoost for big data: an interdisciplinary review. Journal of Big Data, 2020. 7(1): p. 94.

[31] P, L., et al., Catboost: unbiased boosting with categorical features. . In S. Bengio, H. Wallach, H. Larochelle, K. Grauman, N. Cesa-Bianchi, and R. Garnett, editors, Advances in Neural Information Processing Systems ,Curran Associates, Inc., 2018: p. 6638–6648.

[32] Dorogush, A.V., Vasily Ershov, and A. Gulin, CatBoost: gradient boosting with categorical features support. arXiv,https://arxiv.org/abs/1810.11363, 2018.

[33] Hussain, B.Z., et al. Wasserstein GAN based Chest X-Ray Dataset Augmentation for Deep Learning Models: COVID-19 Detection Use-Case. in 2022 44th Annual International Conference of the IEEE Engineering in Medicine & Biology Society (EMBC). 2022.

[34] Ciano, G., et al., A Multi-Stage GAN for Multi-Organ Chest X-ray Image Generation and Segmentation. 2021. 9(22): p. 2896.

[35] Motamed, S., P. Rogalla, and F. Khalvati, Data augmentation using Generative Adversarial Networks (GANs) for GAN-based detection of Pneumonia and COVID-19 in chest X-ray images. Inform Med Unlocked, 2021. 27: p. 100779.